# Chemical Environment Selectivity in Mössbauer Diffraction from $^{57}Fe_3Al$

T. A. Stephens and B. Fultz

*Division of Engineering and Applied Science, mail 138-78, California Institute of Technology, Pasadena, California 91125*

(Received 5 March 1996)

Mössbauer diffraction was used to measure different autocorrelation functions for $^{57}Fe$ atoms in different chemical environments. The sample was polycrystalline $^{57}Fe_3Al$ with the ordered $DO_3$ structure. Diffraction peaks from a fcc structure with a doubled unit cell were detected when the incident radiation was tuned to the Mössbauer resonance of the Wyckoff 4(b) Fe site, but not for tuning to the 8(c) site, thereby distinguishing the spatial arrangements of these two Fe sites. [S0031-9007(96)02020-0]

PACS numbers: 76.80.+y, 07.85.Nc, 61.10.Eq

Most of what we know about atomic arrangements in materials has been learned from diffraction experiments. Three coherent scattering processes have proved useful: scattering of x rays by atomic electrons, scattering of electrons from Coulombic interactions with the electronic and nuclear charge of the atom, and scattering of neutrons from nuclei or magnetic electrons. Some Mössbauer scattering processes are coherent and may be useful for diffraction experiments on materials. Coherent interference between x-ray and Mössbauer scattering was first identified in Mössbauer energy spectra [1,2]. Later experiments with high quality single crystals measured diffraction peaks directly [3–5]. These later studies showed that with strong dynamical diffraction there is a suppression of incoherent decay channels such as internal conversion processes, and a large lifetime broadening of peaks in the Mössbauer energy spectra [6–12].

In this Letter, we show a new feature of Mössbauer diffraction that is useful for studies of atomic arrangements in materials—we show that Mössbauer diffraction can measure the autocorrelation function of $^{57}Fe$ atoms as a functional of their chemical environment. By working with polycrystalline materials near the kinematical limit of diffraction, the broadening of nuclear energy levels is not severe, so the spectroscopic capabilities of Mössbauer scattering are preserved. The structure of the bcc-based $DO_3$ structure is shown in Fig. 1. The two sites for the $^{57}Fe$ atoms, the Wyckoff 4(b) and 8(c) sites, differ in both their chemical environment (0 versus 4 Al neighbors) and in their spatial arrangement (face-centered cubic, fcc, with lattice parameter $2a_0$ versus simple cubic, sc, with lattice parameter $a_0$). In the present experiment, we tuned the incident beam to the hyperfine magnetic field (HMF) of each chemical environment (0 Al and 4 Al), and detected diffraction peaks characteristic of their spatial arrangements (fcc and sc).

Pieces of $^{57}Fe$ (95% isotopically enriched) and Al metal were arc melted under an argon atmosphere and remelted several times to ensure homogeneity. The 50 mg ingot was then induction melted and splat quenched in high vacuum to obtain a chemically disordered foil of 35 $\mu$m thickness. This foil was cold-rolled to a thickness of 3 $\mu$m. To obtain $DO_3$ chemical order, the samples were annealed in evacuated quartz ampoules at 773 K for 6 days, followed by 723 K for 40 days. X-ray diffractometry showed $(\frac{1}{2}\,\frac{1}{2}\,\frac{1}{2})$ and (1 0 0) diffraction peaks indicative of a high degree of chemical order in the alloy, but the strong rolling texture of the foil made it impossible to quantify the long range order (LRO) parameter. However, similar heat treatment procedures on filed powders produced LRO parameters of close to unity. A JEOL superprobe 733 electron microprobe was used to check for chemical heterogeneities and to determine that the chemical composition of the foil was Fe-25.4 at. % Al. Conversion electron Mössbauer spectrometry results, reported below, showed a high degree of short-range order. X-ray diffractometry showed that the foil had a strong crystallographic texture with (1 1 1) and (1 0 0) planes parallel to the plane of the rolled foil, as is typical of bcc Fe [13].

The experiment required the development of a Debye-Scherrer powder diffractometer for Mössbauer scattering (Fig. 2), which was built around an Inel CPS-120 large angle position-sensitive detector (PSD). The background count rate was 3.5 Hz over the entire detector with no source present. (The overall count rate doubled with the sample in position but with the incident beam blocked from entering the detector.) Our instrument differs from rocking curve diffractometers appropriate for

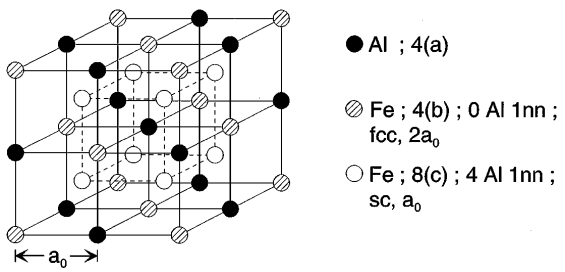


FIG. 1. The $DO_3$ ordered structure of $Fe_3Al$, the three crystallographic sites, and their spatial arrangement.

 0031-9007/97/78(2)/366(4)$10.00 

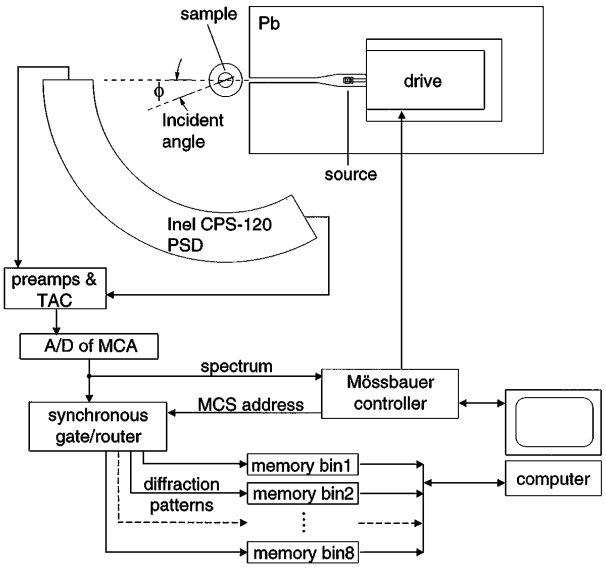


FIG. 2. Schematic of our Mössbauer powder diffractometer.

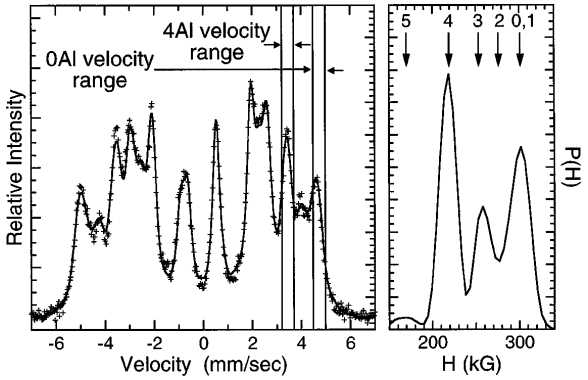


FIG. 3. Left, conversion electron Mössbauer spectrum of partially $DO_3$ ordered $^{57}Fe_3Al$ samples used in the present experiment. Vertical lines indicate the range of tuning of the Doppler drive for obtaining the diffraction patterns in Fig. 4. Right, HMF distribution.

single crystal work [6–12], or powder diffractometers designed to measure energy spectra [14–16]. An earlier version of this instrument was used to make the first measurements of diffraction patterns from polycrystalline bcc $^{57}Fe$ [17]. The present system had a precision set of collimation slits and a source of $^{57}Co$ in Rh with an initial activity of 140 mCi. The Doppler drive was operated in a region-of-interest mode around selected peaks in the energy spectrum, and the electronics provided for the collection of independent diffraction patterns from up to eight subranges in energy. For the bcc fundamental diffractions, we studied interferences of x-ray and Mössbauer scattering, and these measurements will be reported elsewhere. For the chemical periodicities of the $DO_3$ structure, however, the x-ray scattering is rather weak, and no significant effects of interference were observed with the quality of the present data. The data here are reported as a sum of all diffraction patterns acquired near resonance, as shown by the energy windows in Fig. 3.

Data collection alternated between the off-resonance condition (using two Doppler velocity ranges: $-27$ to $-8$ and $+8$ to $+27$ mm/sec) and the two resonance conditions shown in Fig. 3. To help compensate for gain variations across the PSD, the PSD was rotated by 2.00°, and data collection was repeated for each resonance condition. This full procedure was repeated after the incident angle, $\phi$, of the specimen was changed by 1.0° intervals near $\phi = 23°$. Data sets were also acquired without a specimen so that the background of the diffractometer could be measured. Times and source activity (varying from 140 to 70 mCi over the course of our measurements) were monitored carefully so that all diffraction patterns could be normalized by the incident flux. Relative values of the incident flux were also determined by measuring the count rate for a few diffraction patterns acquired when the transmitted beam was allowed into the detector. The resonance conditions were also checked with the spectra acquired in this condition. Owing to a differential nonlinearity in the least significant bit of the analog-digital converter, it was necessary to smooth the data with a running average of adjacent data points.

A conversion electron Mössbauer spectrum of the $^{57}Fe_3Al$ specimen is presented in Fig. 3. Alloys of $Fe_3Al$ have been studied extensively by Mössbauer spectrometry, and interpretations of their spectra are well established [18–21]. In essence, the $^{57}Fe$ HMF is decreased as the $^{57}Fe$ atom has an increasing number of Al atoms in its first-nearest-neighbor (1 nn) shell. The HMF distribution, extracted from the spectrum by the method of Le Caër and Dubois [22], is presented in Fig. 3. The HMF's for each chemical environment are labeled at the top of the figure with the number of Al atoms in the 1 nn shell of the $^{57}Fe$ atom. In particular, the HMF for $^{57}Fe$ atoms with zero Al neighbors is approximately 310 kG, and for four Al neighbors it is 215 kG. From studies of chemical ordering in $Fe_3Al$ and related alloys, it is well established that the HMF's for these two chemical environments do not change with disorder in the alloy [21]. Figure 3 also shows how the "on-resonance" conditions were selected at the sixth peaks ($m = -\frac{1}{2} \rightarrow -\frac{3}{2}$) of the ferromagnetic sextets of the 0 Al and 4 Al environments.

The diffraction pattern at the top of Fig. 4 is the sum of the data collected at all resonance conditions (0 Al, 4 Al, and off). It shows two prominent bcc fundamental diffractions, the (211) and (222), although the (220) is missing owing to the crystallographic texture induced by cold rolling. This texture makes it impractical to compare the intensities of diffractions from different crystallographic planes. The change in intensity of an individual

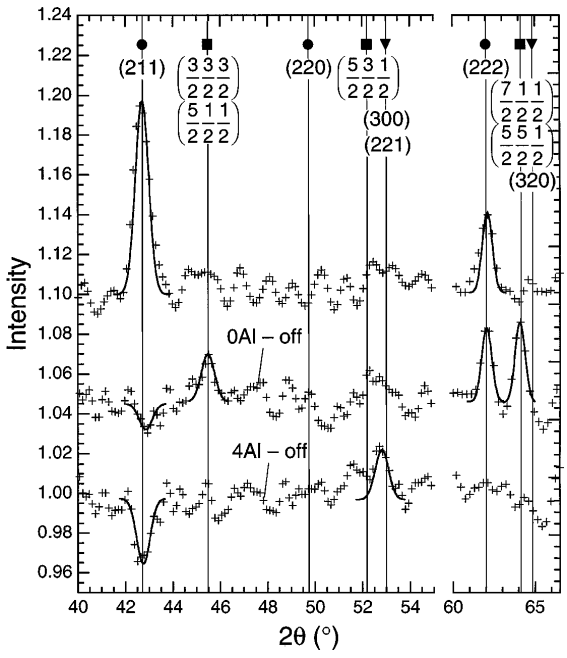


FIG. 4. Top, sum of diffraction patterns for all tunings of the Doppler drive, corrected for instrument background. Gaussian peaks of width consistent with polycrystalline Si diffractions are fit to the experimental peaks. Middle, difference of the diffraction patterns obtained with the drive tuned to the 0 Al environment and the drive detuned off resonance. Circles, peaks expected from bcc structure (also sc, fcc of $2a_0$); triangles, peaks expected from sc (also fcc of $2a_0$); squares, peaks expected from fcc of $2a_0$.

peak caused by changing the resonance conditions should, however, be reliable.

The differential diffraction pattern in the middle of Fig. 4 is the diffraction pattern obtained with the incident beam tuned for the 0 Al environment, minus the diffraction pattern obtained in the off-resonance condition. The middle data set shows strong intensities at the positions of the $(\frac{3}{2}\,\frac{3}{2}\,\frac{3}{2})$, $(\frac{5}{2}\,\frac{1}{2}\,\frac{1}{2})$, and $(\frac{7}{2}\,\frac{1}{2}\,\frac{1}{2})$, $(\frac{5}{2}\,\frac{5}{2}\,\frac{1}{2})$ diffraction peaks. From counting statistics, our confidence in the $(\frac{7}{2}\,\frac{1}{2}\,\frac{1}{2})$, $(\frac{5}{2}\,\frac{5}{2}\,\frac{1}{2})$ differential diffraction peak in the middle data set of Fig. 4 is $3\sigma$, our confidence in the $(\frac{3}{2}\,\frac{3}{2}\,\frac{3}{2})$, $(\frac{5}{2}\,\frac{1}{2}\,\frac{1}{2})$ differential diffraction peak is $2\sigma$. There are about 350 and 250 counts in these two peaks, respectively. (We have two other data sets, not added to these here, which show similar $(\frac{3}{2}\,\frac{3}{2}\,\frac{3}{2})$, $(\frac{5}{2}\,\frac{1}{2}\,\frac{1}{2})$ peaks with confidence levels of $2\sigma$ and $1.2\sigma$.) The bottom data set is a difference of diffraction patterns from the 4 Al environment, minus the diffraction pattern collected in the off-resonance condition. The "half-integral" diffraction peaks are obviously much weaker for the bottom data set. The half-intergral diffraction peaks are expected from a fcc lattice of lattice parameter $2a_0$, although not from a sc or a bcc lattice of lattice parameter $a_0$. Figure 4 therefore demonstrates the chemical environment selectivity of Mössbauer diffraction. Chemical environment selectivity differs from the chemical selectivity of isomorphous substitution or anomalous scattering of x rays, since our method differentiates between chemical environments of the same atom. Because of the crystallographic texture of the sample, our evidence is less convincing for the trends of the (300), (221) differential diffraction peak. This peak is expected to be twice as strong in the 4 Al diffraction pattern than in the 0 Al diffraction pattern, because there are twice as many $^{57}$Fe atoms with the 4 Al chemical environment.

The kinematical intensity of diffraction at a particular $\Delta\mathbf{k}$ and $E$ is the Fourier transform of the Patterson function, $P(\mathbf{r}, E)$ [23]:

$$I(\Delta\mathbf{k}, E) = \sum_{\mathbf{r}=-\infty}^{\infty} e^{i\Delta\mathbf{k}\cdot\mathbf{r}} P(\mathbf{r}, E)\,, \tag{1}$$

where the sum over $\mathbf{r}$ includes all atom sites of the crystal. The Patterson function is a spatial autocorrelation function of the Mössbauer scattering factor distribution,

$$P(\mathbf{r}, E) = \sum_{\mathbf{r}'=-\infty}^{\infty} \sum_{i} \sum_{\Delta=I}^{6} \sum_{j} \sum_{\Delta'=1}^{6} f^*(\mathbf{r}', \varepsilon_i^{\Delta}, E) \times f(\mathbf{r}' + \mathbf{r}, \varepsilon_i^{\Delta'}, E)\overline{P}(\Delta, \Delta')\,. \tag{2}$$

Chemical environments that cause different hyperfine interactions are denoted by $i$ and $j$ in Eq. (2), which includes explicitly the six nuclear transitions of $^{57}$Fe in a HMF. The polycrystalline-averaged polarization factor, $\overline{P}(\Delta, \Delta')$, is small when $\Delta \neq \Delta'$ [15]. The Mössbauer scattering factor, $f(\mathbf{r}, \varepsilon_i^{\Delta}, E)$, is strongly energy dependent as

$$f(\mathbf{r}, \varepsilon_i^{\Delta}, E) = -G_i^{\Delta}\rho(\mathbf{r}, i)\left(\frac{1}{2(E - \varepsilon_i^{\Delta})/\Gamma + i}\right). \tag{3}$$

where the factor $G_i^{\Delta}$ includes all information about the Mössbauer transition probability such as spin levels, internal conversion coefficient, Clebsch-Gordon coefficients, and Lamb-Mössbauer factors [5,6,9]. Here $\rho(\mathbf{r}, i)$ is the probability of finding a $^{57}$Fe nucleus with chemical environment, $i$, at position $\mathbf{r}$. The last factor in Eq. (3) describes how the phase of scattering depends on $E$, and is largest when $E$ is at resonance. Here $\Gamma$ is the natural linewidth. Equation (2) allows only for interference between waves scattered by different nuclei. Consideration of coherent x-ray scattering is not as important for interpreting our results on chemical environment selectivity, since x-ray superlattice diffractions such as $(\frac{3}{2}\,\frac{3}{2}\,\frac{3}{2})$ are weak.

Chemical environment selectivity in Mössbauer diffraction will be most effective when the environments differ strongly in their energy levels ($\varepsilon_i^{\Delta} - \varepsilon_j^{\Delta}$ should be large, except when $i = j$). This is a reasonable approximation for the 0 Al and 4 Al environments, which are separated in energy by $6.3\Gamma$. Although there is a strong overlap in energy of the scattering factors of the 0 Al and 1 Al environments, most of the $^{57}$Fe atoms with the 1 Al chemical environment are expected to be 4(b) Fe atoms with an antisite Al neighbor. The spatial autocorrelation function

of the 1 Al environment is therefore probably similar to that of the 0 Al environment. The $m = -\frac{1}{2} \rightarrow -\frac{1}{2}$ transition for the 0 Al environment is separated in energy by $4.4\Gamma$ from the $m = -\frac{1}{2} \rightarrow -\frac{3}{2}$ transition from the 4 Al environment. This overlap of spectral peaks will cause only a small amount of a fcc diffraction pattern to appear in our resonance condition for the 4 Al environment, since there are fewer 0 Al environments than 4 Al environments. Furthermore, only half of the scatterings from the $m = -\frac{1}{2} \rightarrow -\frac{1}{2}$ transition can be coherent [5], suppressing the intensity of the diffraction peak by a factor of 4.

Although the present experiment was made possible by the position-sensitive detector, the detector brought serious technical limitations. At $2\theta = 50°$, the geometrical efficiency of the detector was less than 1%. The count rate for coherent Mössbauer scattering was only 0.25% as large as the count rate from background and x-ray fluorescences. The detector efficiency for 14.41 keV photons was 15%. Energy resolution and better geometrical efficiency of the detector should permit significant improvements in Mössbauer powder diffractometry with collimated radioisotope sources. Mössbauer diffraction experiments with synchrotron radiation sources are possible in the time domain, although monochromatic, highly polarized photons have recently been generated with a synchrotron source [24].

This work was supported by the U.S. National Science Foundation under Contract No. DMR-9415331.

[1] P. J. Black and P. B. Moon, Nature (London) **188**, 481 (1960).
[2] P. J. Black, G. Longworth, and D. A. O'Connor, Proc. Phys. Soc. **83**, 925 (1964).
[3] P. J. Black and I. P. Duerdoth, Proc. Phys. Soc. **84**, 169 (1964).
[4] G. V. Smirnov, V. V. Sklyarevskii, R. A. Voskanyan, and A. N. Artem'ev, Zh. Eksp. Teor. Fiz. Pis'ma Red. **9**, 123 (1969).
[5] V. A. Belyakov, Usp. Fiz. Nauk. **115**, 553 (1975).
[6] U. van Bürck, G. V. Smirnov, R. L. Mössbauer, F. Parak, and N. A. Semioschkina, J. Phys. C **11**, 2305 (1978).
[7] U. van Bürck, R. L. Mössbauer, E. Gerdau, R. Rüffer, R. Hollatz, G. V. Smirnov, and J. P. Hannon, Phys. Rev. Lett. **59**, 355 (1987).
[8] Y. V. Shvyd'ko and G. V. Smirnov, J. Phys. Condens. Matter **1**, 10 563 (1989).
[9] J. Arthur, G. S. Brown, D. E. Brown, and S. L. Ruby, Phys. Rev. Lett. **63**, 1629 (1989).
[10] J. B. Hastings, D. P. Siddons, and M. Lehmann, Phys. Rev. Lett. **64**, 2030 (1990).
[11] P. P. Kovalenko, V. G. Labushkin, A. K. Ovsepyan, E. R. Sarkisov, E. V. Smirnov, and I. G. Tolpekin, Zh. Eksp. Teor. Fiz. **88**, 1336 (1985) [Sov. Phys. JETP **61**, 793 (1985)].
[12] H. Winkler, R. Eisberg, E. Alp, R. Rüffer, E. Gerdau, S. Lauer, A. X. Trautwein, M. Grodzicki, and A. Vera, Z. Phys. B **49**, 331 (1983).
[13] C. S. Barrett, *Structure of Metals* (McGraw-Hill, New York, 1943) pp. 405–406.
[14] Y. Nakai, M. Hirano, Y. Ooi, and N. Kunitomi, J. Phys. Soc. Jpn. **51**, 929 (1982).
[15] Y. Nakai, Y. Ooi, and N. Kunitomi, J. Phys. Soc. Jpn. **57**, 3172 (1988).
[16] M. Tegze and G. Faigel, Hyperfine Interact. **92**, 1143 (1994).
[17] T. A. Stephens, W. Keune, and B. Fultz, Hyperfine Interact. **92**, 1095 (1994).
[18] S. A. Losievskaya, Phys. Status Solidi (a) **16**, 647 (1973).
[19] G. Athanassiadis, G. Le Caër, J. Foct, and L. Rimlinger, Phys. Status Solidi (a) **40**, 425 (1977).
[20] J. E. Frackowiak, Phys. Status Solidi **87**, 109 (1985); Hyperfine Interact. **28**, 1067 (1986).
[21] B. Fultz and Z. Q. Gao, Nucl. Instrum. Methods Phys. Res. Sect. B **76**, 115 (1993); Z. Q. Gao and B. Fultz, Philos. Mag. B **67**, 787 (1993).
[22] G. Le Caër and J. M. Dubois, J. Phys. E **12**, 1083 (1979).
[23] J. M. Cowley, *Diffraction Physics* (North-Holland, Amsterdam, 1975), Sec. 5.3.
[24] G. V. Smirnov, U. van Bürck, A. I. Chumakov, A. Q. R. Baron, and R. Rüffer (to be published).